第 33 卷第 12 期　　焊　接　学　报　　Vol. 33　No. 12
2012 年 12 月　　TRANSACTIONS OF THE CHINA WELDING INSTITUTION　　December　2012

新型铝合金薄板对接激光焊接头性能

占小红[1,2]，　陈　洁[1]，　陶　汪[3]，　杨志斌[3]，　魏艳红[2,3]，　陈彦宾[3]，　欧文敏[2]

（1. 中国商飞上海飞机制造有限公司，上海 200436；2. 南京航空航天大学 材料科学与技术学院，南京　210016；
3. 哈尔滨工业大学 现代焊接生产技术国家重点实验室，哈尔滨　150001）

占小红

摘　要：以 6156 铝合金为主要研究对象，对比了其激光填丝焊与自熔焊各自特点，探讨了焊缝表面成形、焊缝熔宽的影响因素及接头的抗拉强度与疲劳强度变化规律. 结果表明，功率在 1 800 W 左右，焊接速度在 2 ~ 3.5 mm/min，送丝速度在 2 ~ 3.5 mm/min 范围能获得较好的焊缝表面成形；接头焊后不经热处理抗拉强度可达 314.3 MPa，为母材强度的 81.3%，且有良好的抗疲劳性能；铝合金激光焊具有焊接速度高、焊缝成形美观、焊接参数范围广的特点，是一种良好的焊接方式.

关键词：激光焊接；铝合金；对接；填丝焊

中图分类号：TG456.7　　**文献标识码**：A　　**文章编号**：0253 - 360X(2012)12 - 0037 - 04

0　序　　言

铝及铝合金激光焊接技术是最近十几年来才发展起来的一项新技术，与传统焊接技术相比，它在焊接质量、效率、可靠性、自动化等各方面都具有无可比拟的优越性.

近年来，随着大功率、高性能激光加工设备的不断研制成功，在工业发达国家的航空制造业中，铝合金激光焊接技术已经进入工程实用阶段[1]. 空中客车公司在 A318，A340，A380 等多种机型上采用了激光焊接的整体机身壁板制造技术取代原有的铆接工艺，极大地减轻了机身重量，并且提高了生产效率、降低了制造成本[2]. 而新型材料 6156 铝合金为 Al-Mg-Si 系列的中高强度铝合金，具有优良的延展性、耐腐蚀性和良好的焊接性，目前正作为国内大型民用客机机身蒙皮的主要备选材料之一. 激光焊接铝合金的技术，经过最近十几年的发展，逐渐成为实现铝合金结构连接最具有技术和经济优势的方法[3,4]. 国内外诸多学者针对铝合金激光焊接组织与性能开展了大量研究[5-7]，而针对 6156 这一新型材料的研究并不多见. 文中针对 6156 机身蒙皮薄板结构，开展激光焊接工艺与性能研究，并重点考察了焊接接头的拉伸与疲劳性能.

收稿日期：2011 - 10 - 09

基金项目：国家自然科学基金资助项目（50904038）；国家商用飞机制造工程技术研究中心创新基金资助项目（SAMC12-JS-15-009）

1　试验方法

采用 1.8 mm 厚的 6156 铝合金薄板进行激光填丝焊接试验，试样尺寸为 320 mm × 40 mm × 1.8 mm，填充焊丝为 ER4047 铝硅合金焊丝，成分见表 1. 焊后对焊缝外观成形进行分析，采用金相显微镜观察分析焊缝显微组织，同时对焊缝的静载和疲劳性能进行测试和分析.

试验所采用的激光器为德国 ROFIN-SINAR 公司生产的射频激励扩散冷却 CO_2 激光器，最大输出功率 3.0 kW，波长 10.6 μm，最小光斑直径 0.15 mm，模式为 TEM01，其能量分布为高斯模式. 试验采用奥地利福尼斯（Fronius）送丝系统，送丝速度在 0.03 ~ 9.99 m/min 范围内精确可调，保证焊丝匀速平稳的送达焊接位置，试验过程中采用高纯度氦气进行保护.

2　试验结果分析

2.1　焊接参数对焊缝成形的影响

2.1.1　送丝速度的影响

送丝速度是填丝激光焊的一个重要工艺参数. 合理选择送丝速度可以充分利用激光能量，提高生产效率. 送丝速度过慢将不能克服激光焊时的穿孔及上表面下塌等缺陷；而送丝速度过快则会导致焊缝下表面下塌，严重时甚至产生柱丝、堆丝等缺陷. 图 1 为在热输入一定的情况下，不同的送丝速度与

表面熔宽、背面熔宽和表面余高的关系.

表1 6156铝合金和ER4047焊丝合金元素成分(质量分数,%)

Table 1 Compositions in Al-alloy 6156 and welding wire ER4047

	Si	Fe	Cu	Mn	Zn	Ti	Mg	Al
6156	1.0	—	0.9	0.6	—	—	0.9	余量
ER4047	11.52	0.20	<0.001	0.01	0.001	0.01	0.01	余量

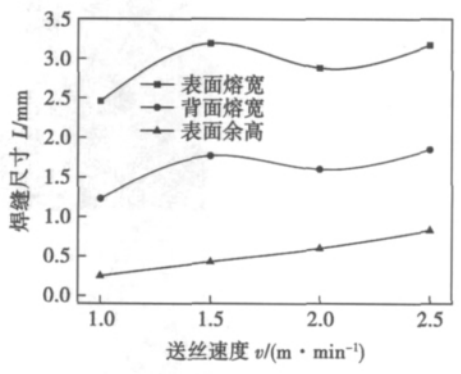

图1 送丝速度与表面熔宽、背面熔宽和表面余高的关系

Fig. 1 Influence of different wire feeding rate on surface width, back width and excess height of weld seam

由图1中可以看出,在热输入一定且送丝速度低于1.6 m/min的情况下,焊缝熔宽随着送丝速度的提高而迅速增加,在送丝速度高于1.6 m/min以后,随着送丝速度的提高,焊缝宽度先减小后增加.这是因为,送丝速度提高一方面使填充金属量增加,有使宽度增加的倾向;但另一方面较多的焊丝熔化需要吸收更多的激光能量,使熔化母材吸收的能量减少,因而有使熔池变窄的倾向.

2.1.2 激光功率和焊接速度的影响

通过试验可以发现,6156铝合金能否有效实现激光深熔焊接与激光功率关系密切,而对焊接速度和送丝量敏感性小.激光功率稍降低二三百瓦则不能焊接,稍高二三百瓦则焊接过程异常不稳定.这是由于铝合金的高热导率和对激光的高反射率,使得铝合金的激光焊接功率需要较高的功率密度.研究表明,当激光功率密度低于某一临界值(功率阈值)时,激光加工表现为热传导焊过程.而功率密度高于这一临界值时,材料表面在激光束的辐射下强烈汽化并形成小孔后,深熔焊接过程便得以实现.经过文中的试验可以发现,功率在1 800 W左右,焊接速度在2~3.5 mm/min范围且送丝速度在2~3.5 mm/min,则能有效且较为稳定地开展焊接.焊缝外观成形如图2所示.

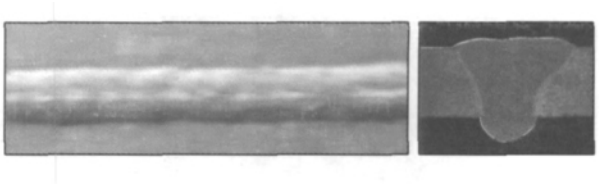

图2 激光填丝焊接焊缝外观及截面形貌

Fig. 2 External appearance and cross section of laser feeding welding

2.2 焊缝的拉伸性能

母材和接头的拉伸试验是在国产电子万能试验机上进行,加载速度为2 mm/min,最大加载载荷为100 kN,试样尺寸依照中华人民共和国航空工业标准HB5143—1996《金属室温拉伸试验方法》制定.

6156铝合金激光焊接头拉伸试验结果见图3.对于填丝焊来说,最大抗拉强度为341.4 MPa,最大抗拉强度达到母材(387.5 MPa)的88.1%;平均抗拉强度为314.3 MPa,为母材的81.3%.而自熔焊接头强度普遍较低,其最大抗拉强度为248.3 MPa,平均抗拉强度196.3 MPa,平均抗拉强度仅为母材的50.65%.填丝焊与自熔焊的屈服强度都仅为母材的50%左右,这是由于6156铝合金母材为T6热处理状态,时效热处理过程中析出的强化相分解且冷却后来不及析出,使接头的屈服强度和断裂强度显著下降.

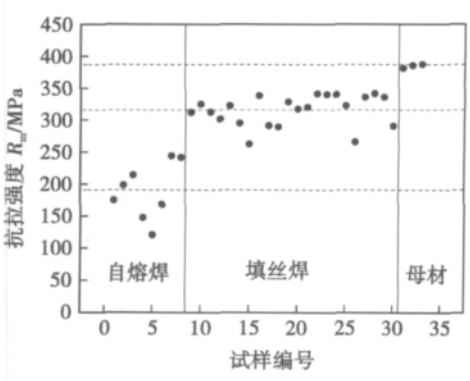

图3 各个参数下的抗拉强度

Fig. 3 Tensile strength with different parameters

6156铝合金激光焊接头拉伸断裂位置如图4所示.此次拉伸共有两种断裂方式:一是沿焊缝中心断裂,如图4a,起裂位置在焊缝中部,然后向焊缝表面拓展,最后拓展到母材的近焊缝区发生断裂,这主要是由于焊缝中部存在有气孔,减少了焊缝的有效承载横截面积,从而降低了该处的承载能力所致.二是沿熔合线断裂,如图4b,这种断裂形式占绝大部分,起裂位置在焊缝焊趾上,这也充分说明熔合线

处是焊缝的薄弱环节.

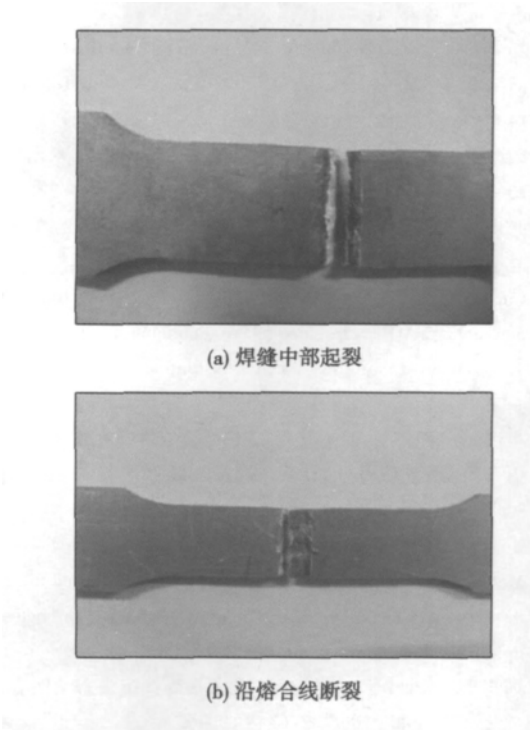

图 4　6156 铝合金激光填丝焊接头拉伸断裂形式

Fig. 4　Fracture form of laser feeding welded joint for 6156 Al-alloy

填丝焊的焊接接头要比自熔焊的焊接接头塑性高,这可以从它们的断后伸长率和断面收缩率看出,见表 2.

表 2　接头的塑性指标

Table 2　Plastic parameter for welded joint

厚度 h/mm	试样种类	断后伸长率 A(%)	断面收缩率 φ(%)
1.8	母材	19.48	12.7
1.8	自熔焊	2.28	7.6
1.8	填丝焊	3.24	8.9

图 5 为 6156 铝合金焊接接头拉伸断口的 SEM 形貌. 由图 5 可知,焊缝断裂为混合特征,起裂区位于焊趾处,表现为准解理形貌,如图 5a; 然后向焊缝扩展,焊缝断口存在着大量的韧窝,如图 5b 所示.

2.3　焊缝的疲劳性能

文中的疲劳试验为高频疲劳,频率为 60 Hz,应力比为 0.1. 结果表明,当最大载荷为 1.8 N 时,平均疲劳周次可达 149 423 次. 但是随着应力水平的降低不存在无限寿命,S-N 曲线没有水平部分.

试件断裂于焊缝中间位置,随着疲劳周次的增加试件萌生裂纹,之后急剧扩展,直接断裂于焊缝的中间位置. 疲劳断口的 SEM 形貌如图 6 所示. 可以发现: 断口的起始位置为撕裂的脆性断裂,焊缝的中

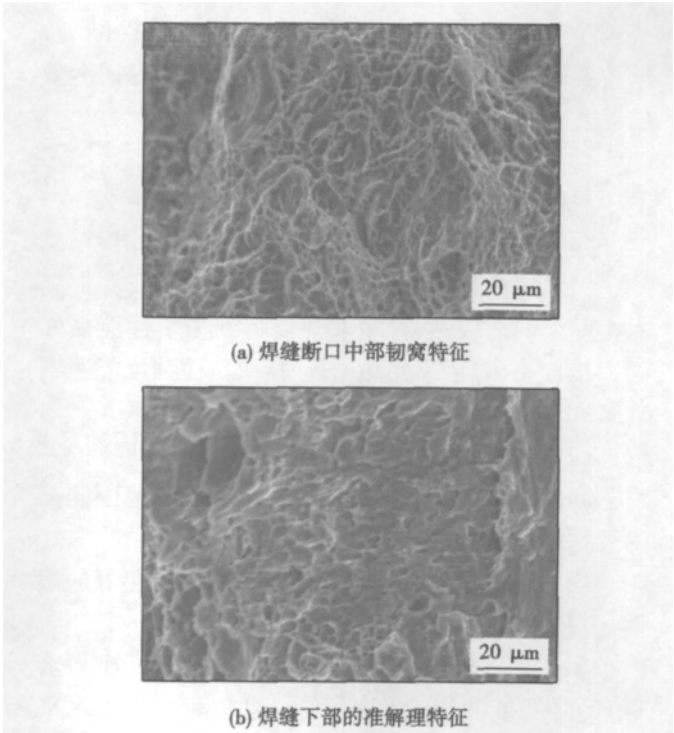

图 5　6156 铝合金激光填丝焊接头拉伸断口 SEM 特征

Fig. 5　Fracture SEM results of laser feeding welded joint for 6156 Al-alloy

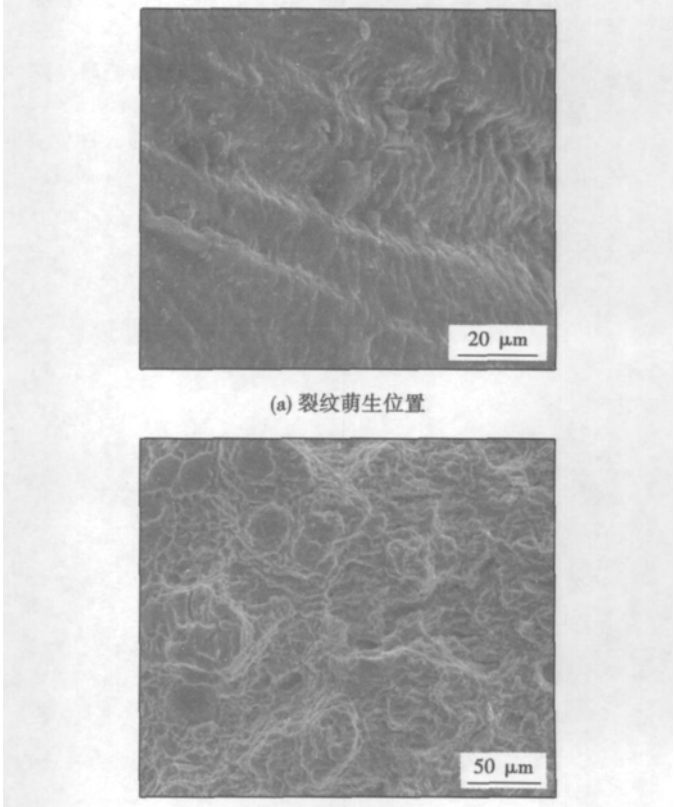

图 6　疲劳断口 SEM 形貌

Fig. 6　SEM results of fatigue fracture

心部位有少量的韧窝，但是主要表现为脆性断裂. 这主要是因为断裂是瞬间发生，来不及形成韧窝就已经发生断裂.

3 结 论

(1) 填丝焊能大大改善焊缝表面成形，并提高对接间隙的适应性，且填丝焊能得到力学性能良好的焊接接头，焊后不经热处理，接头抗拉强度能达到6156 母材的 80% 以上.

(2) 激光功率在 1 800 W 左右，焊接速度在 2 ~ 3.5 mm/min，送丝速度在 2 ~ 3.5 mm/min 范围能获得较好的焊缝表面成形.

(3) 填丝焊的接头较自熔焊接头具有更好的塑性，但相对于母材来说其塑性都有所降低.

(4) 疲劳寿命的特点是随着最大载荷(应力水平)的降低疲劳周次不断增加，但是随着应力水平的降低不存在无限寿命.

参考文献:

[1] Norris I. Laser welding developments [J]. Welding Review, 1998 (4): 20 - 22.

[2] 肖荣诗，陈 铠，左铁钏. 高强铝合金激光焊接新进展 [J]. 应用激光，2002，22(2)：206 - 208.
Xiao Rongshi, Chen Kai, Zuo Tiechuan. Development of laser beam welding of high strength aluminum alloys [J]. Applied Laser, 2002, 22(2): 206 - 208.

[3] 朱 宏，金忠华. 铝及铝合金激光焊接技术的研究现状 [J]. 电子工艺技术，1997，18(4)：129 - 132.
Zhu Hong, Jin Zhonghua. State of the art of laser welding for aluminum and aluminum alloys [J]. Electronics Process Technology, 1997, 18(4): 129 - 132.

[4] 陈彦宾. 现代激光焊接技术 [M]. 北京：科学技术出版社，2005.

[5] 崔 丽，李晓延，贺定勇，等. 5A90 铝锂合金激光焊焊缝微观组织特征 [J]. 焊接学报，2010，31(9)：94 - 96.
Cui Li, Li Xiaoyan, He Dingyong, *et al*. Microstructure investigation of Nd: YAG laser welded 5A90 aluminium-lithium alloys [J]. Transactions of the China Welding Institution, 2010, 31(9): 94 - 96.

[6] 牛锐锋，林冰华，王亚妮，等. 铝合金脉冲激光焊 Mg 元素烧损行为及接头硬度分布 [J]. 焊接学报，2010，31(3)：81 - 83.
Niu Ruifeng, Lin Binghua, Wang Yani, *et al*. Evaporation loss of Mg element in pulsed laser welding of 5A05 aluminum alloy and distribution of micro-hardness of welding joint [J]. Transactions of the China Welding Institution, 2010, 31(3): 81 - 83.

[7] 周清林. 铝合金 CO_2 激光与 TIG 薄板焊接接头力学性能分析 [J]. 焊接学报，2006，27(8)：63 - 65.
Zhou Qinglin. Mechanical properties of CO_2-laser and TIG aluminium alloy welded joint [J]. Transactions of the China Welding Institution, 2006, 27(8): 63 - 65.

作者简介： 占小红，男，1979 年出生，博士后，副教授. 主要从事航空制造工艺、焊接过程数值模拟及仿真、焊接工程软件等研究工作. 发表论文 20 余篇. Email: xhzhan@nuaa.edu.cn

Abstract: TCS345, T4003, Nirosta 4003 and JFE410RW ferritic stainless steels were welded by ER-309 welding wire in this paper. The microstructure of their base metal and joint were analyzed by metallographic approach, and the corrosion resistance of base metal and joints was evaluated by electrochemical corrosion tests. The experimental results demonstrated that, compared with that of Nirosta 4003 and JFE410RW, low content of Ti and Mn elements were found in TCS345 and T4003 ferritic stainless steels, especially the low content of Ti, which resulted in the obvious grain growth of TCS345 and T4003 ferritic stainless steels. Moreover, the welding joints of ferritic stainless steels exhibited big heat affected zone (HAZ). Compared with the microstructure of base metal, the HAZ area showed obvious large grains. As far as TCS345 is concerned, obvious grain growth is observed. In the case of Nirosta 4003 and JFE410RW, they exhibited smaller size of grain than TCS345. In 1mol/L Na_2SO_4 solution, the corrosion resistance of TCS345 and JFE410RW is better than that of T4003 and Nirosta 4003.

Key words: ferritic stainless steel; welding joint; metallographic microstructure; corrosion resistance

Effect of microplasma spraying working gas on crystallinity of HA coatings ZHAO Qiuying[1], HE Dingyong[2], LIU Yan[2], LI Xiaoyan[2], CHEN Shujun[3] (1. Postdoctoral Research Station of Mechanical Engineering, Beijing University of Technology, Beijing 100124, China; 2. College of Materials Science and Engineering, Beijing University of Technology, Beijing 100124, China; 3. College of Mechanical Engineering and Applied Electronics Technology, Beijing University of Technology, Beijing 100124, China). pp 23 - 27

Abstract: Hydroxyapatite (HA) coatings were prepared on Ti-6Al-4V substrate by using the method of microplasma spraying. Commercially pure argon gas and helium/argon (50% in volume) mixed gas were used as working gas in the spraying processing respectively. The surface morphology, phase compositions and degree of crystallinity of the coatings were examined by scanning electron microscope (SEM) and X-ray diffraction (XRD). Results show that less impurity phases and no TTCP and CaO phases were found in the coatings. The crystallinity of coatings is higher than 70%, which is beneficial for implantation materials stability in vitro and vivo. The enthalpy of microplasma arc in which helium/argon mixed is used as working gas is higher than that in which commercially pure argon gas is used. The crystalline phases in the former coatings mainly consist of recrystallization grains while the latter coatings were mainly made up of lots of unmelted HA particles.

Key words: microplasma spraying; hydroxyapatite coatings; helium/argon mixed gas; crystallinity

Development of hybrid laser + double wire MIG/MAG welding system and process ZHU Yanli[1], LI Huan[1], YANG Lijun[1], GAO Ying[2] (1. Tianjin Key Laboratory of Advanced Joining Technology, Tianjin University, Tianjin 300072, China; 2. Tianjin Key Laboratory of High Speed Cutting and Precision Machining, Tianjin University of Technology and Education, Tianjin 300222, China). pp 28 - 32

Abstract: In order to study the process of laser + double wire welding, the hybrid laser + double wire MIG/MAG welding system was constructed. The method of pulsed controlling of the powers which are mutually independent is alternative. The welding experiments were also carried out with this system in this paper. The double current signals, voltage signals and high-speed camera signals were synchronously collected. The result shows that the hybrid laser + double wire MIG/MAG welding system can carry out stable welding and the appearance of the weld is good. The diversifications of voltage signals were obvious and the stability of voltage signals was improved as a result of injection of the laser power.

Key words: hybrid laser + double wire MIG/MAG welding; electric signals; high-speed camera

Effect of TGO topography on TBCs residual stresses HAN Zhiyong, ZHANG Hua, WANG Zhiping (Tianjin Key Laboratory for Civil Aircraft Airworthiness and Maintenance, Civil Aviation University of China, Tianjin 300300, China). pp 33 - 36

Abstract: By using nonlinear finite element model, the residual stress distribution which was affected by interface topography of top ceramic coat (TCC), bond coat (BC) and thermally-growth oxide (TGO) interface area in thermal barrier coatings (TBCs) system was calculated. In the process of calculation, thermodynamic parameters of TCC, TGO and BC were considered. The calculating results show that the residual stress of TGO interface is affected by interface topography unit size and topography distribution density obviously. The stress on TCC/TGO interface is greater than that on BC/TGO interface. Stress concentrates at the tip of cone topography center and reaches the maximum value, which becomes the dangerous point for failure of thermal barrier coatings system. The residual stress level decreases with the increasing of topography quantity.

Key words: thermal barrier coatings; nonlinear calculation; interface topography; TGO

Study on performance of 6156 skin butt joint with laser beam welding ZHAN Xiaohong[1,2], CHEN Jie[1], TAO Wang[3], YANG Zhibin[3], WEI Yanhong[2,3], CHEN Yanbin[3], OU Wenmin[2] (1. Shanghai Aircraft Manufacturing Co., Ltd, Shanghai 200436, China; 2. College of Material Science and Technology, Nanjing University of Aeronautics and Astronautics, Nanjing 210016, China; 3. State Key Laboratory of Advanced Welding Production Technology, Harbin Institute of Technology, Harbin 150001, China). pp 37 - 40

Abstract: The laser beam welding characteristics of 6156 aluminum butt joint with and without filling wire are investigated. The factors which influence the weld appearance and weld width are analyzed. The variety rule of tensile and fatigue strength are discussed. The results show that the appearance of the weld joint with filler metal is better than the one without filler metal. The maximum weld gap tolerance of the weld joint with filler metal increases to 0.7 mm. The strength of weld joint without heat treatment is 314.3 MPa which is 81.3% of base metal. Laser welding of aluminum is a favorable weld technology with the characteristics of high speed, fine weld appearance and wide weldability.

Key words: laser beam welding; aluminum alloy; butt

joint; filling weld

Analysis and prevention of cracks in laser-welded joint of TiNi shape memory alloy and stainless steel LI Hongmei[1], SUN Daqian[1], DONG Peng[1], CAI Xiaolong[2] (1. School of Materials Science and Engineering, Jilin University, Changchun 130025, China; 2. State Key Laboratory of Rare Earth Resources Utilization, Changchun Institute of Applied Chemistry, Changchun 130022, China). pp 41 - 44

Abstract: Dissimilar metal joints of TiNi shape memory alloy wire and stainless steel wire were welded by laser welding method. The cracks feature and fracture surface morphology of joints were examined by using scanning electron microscopy (SEM) and confocal laser scanning microscope (CLSM). The mechanism of crack formation were analyzed, and some measurements were taken to control the welding cracks. The results showed that the micro-cracks usually emerged in the center of the weld zone and fusion zone of TiNi alloy side. The existence of a large number of brittle compounds in the weld was internal cause of cracks, and the joint subjected to tensile stress was the necessary condition of cracks. The cracking susceptibility can be improved to a certain extent by adding Ni interlayer, Co interlayer, changing the laser beam position, applying an axial force to weld zone and optimizing the laser welding parameters. Adding metal interlayer was a more effective method. The tensile strength reached 372 MPa and 347 MPa respectively by using Ni and Co interlayer, and the joint strength increased by 98.9% and 85.6% respectively, compared with the joint without metal interlayer.

Key words: TiNi shape memory alloy wire; stainless steel wire; laser welding; cracks

Experimental analysis on fusion ratio and composition uniformity of laser hot wire welds ZHENG Shiqing[1], WEN Peng[1,2], SHAN Jiguo[1,2] (1. Department of Mechanical Engineering, Tsinghua University, Beijing 100084, China; 2. Key Lab for Advanced Materials Processing Technology, Ministry of Education, Beijing 100084, China). pp 45 - 48, 72

Abstract: Ductile cast iron is welded with filling stainless steel hot wire in this article, then fusion ratio and distribution of elements are studied. The fusion ratio is as low as 38%-55%. The composition of filler wire distributes in welds uniformly. Nonuniform degrees of element Cr and Ni are 0.5% and 6%. Compared with laser hot wire welding, the fusion ratio of laser-MIG hybrid welds is 69%-77%, and the nonuniform degrees of element Cr and Ni are not less than 62% and 51%. The low electric energy input and its high utilization ratio for heating filler wire contribute to lower fusion ratio in laser hot wire welding compared to laser-MIG hybrid welding. The uniform distribution of filler wire in laser hot wire welds results from the low fusion ratio and solid filler wire transfer.

Key words: laser hot wire welding; laser-MIG hybrid welding; fusion ratio; distribution of elements; ductile cast iron

Joint microstructure and isothermal solidification modeling during transient liquid-phase bonding of a duplex stainless steel YUAN Xinjian[1], LUO Jun[1], TANG Kunlun[1], LI Jia[1], KANG Chungyun[2] (1. College of Materials Science and Engineering, Chongqing University, Chongqing 400044, China; 2. Department of Materials Science and Engineering, Pusan National University, Busan 609735, Korea). pp 49 - 52

Abstract: An experimental investigation on transient liquid-phase bonding of a duplex stainless steel was carried by using Ni-based amorphous alloy as the interlayer. The microstructure of the bonded joint was observed with field emission scanning electron microscope (FE-SEM). The chemical compositions were analyzed by energy-dispersive X-ray spectroscopy (EDS) and wavelength-dispersive spectrometry (WDS). Phase structure of the bonded joint was identified by using X-ray diffraction (XRD). The results indicated that before the completion of isothermal solidification, the major secondary-phase precipitate present in the interface region between the insert and base alloy was BN. The dominating phases appeared in the interlayer zone were γ-Ni solid solution, Ni_3B and Cr-borides. Additionally, three diffusion models were employed to calculate the completion time of the isothermal solidification. By contrast to experimental results, the value obtained by solute distribution model was close to the actual value, and this model was considered to be suitable to the bonding process.

Key words: duplex stainless steel; Ni-based amorphous alloy; transient liquid-phase; microstructure; isothermal solidification

Affecting factors of forming spiking of titanium alloy electron beam deep penetration welding SHI Mingxiao[1], ZHANG Binggang[2], MA Jilong[2], CHEN Guoqing[2], FENG Jicai[2], FAN Ding[1] (1. State Key Laboratory of Gansu Advanced Non-ferrous Metal Materials, Lanzhou University of Technology, Lanzhou 730050, China; 2. State Key Laboratory of Advanced Welding and Joining, Harbin Institute of Technology, Harbin 150001, China). pp 53 - 56

Abstract: The spiking is the unique defect of electron beam welding, which has a serious impact on the welding quality. The academia still hadn't had an unified understanding of the forming mechanism of spiking. To study the forming mechanism of spiking, the orthogonal test was used to carry out the experiment of titanium alloy electron-beam deep-penetration welding. The X-ray detection was done for each weld after welding The results of X-ray detection show that the spiking only exists in the partial penetration weld, and the spiking is the irregular-slited shape while the roots are round. The optical microscope and scanning electron microscope combined with energy dispersion spectroscopy were used to analyze the formation mechanism of spiking. The results show that the pulse of electron beam is the direct cause of spiking formation and the metal vapor with high saturated vapor pressure accelerates the tendency of forming spiking. It is important intrinsic motivation to the generation of spiking.

Key words: electron beam welding; metal vapor; spiking

Effect of trace calcium on performance of AgCuZn alloy BAO Li[1], LONG Weimin[1], ZHANG Guanxing[1], SUI Fangfei[2], LI Hao[2], MA Jia[2] (1. State Key Laboratory of Advanced Brazing Filler Metals and Technology, Zhengzhou Institute of